ECS Journal of Solid State Science and Technology, **3** (2) R5-R8 (2014)
2162-8769/2014/3(2)/R5/4/$31.00 © The Electrochemical Society

The Formation of Smooth Facets on Wet-Etched Patterned Sapphire Substrate

Yu-Chung Chen,[a] Bo-Wen Lin,[a,b] Wen-Ching Hsu,[c] and YewChung Sermon Wu[a,z]

[a]*Department of Materials Science and Engineering, National Chiao Tung University, Hsinchu, Taiwan*
[b]*Crystalwise Technology Inc., Hsinchu, Taiwan*
[c]*Sino-American Silicon Products Inc., Hsinchu, Taiwan*

In this study, rectangle-shaped SiO_2 hard masks with various orientations were employed to find various facets on wet-etched patterned sapphire substrate (PSS). Seven facets (A, B, B_1, B_2, D_1, D_2 and E) were observed after etching. The surfaces of A, B and E-facets were smooth. Their plane indexes were $\{13\bar{4}7\}$, $\{10\bar{1}4\}$ and $\{12\bar{3}5\}$, respectively. On the other hand, the surfaces of B_1, B_2, D_1 and D_2-facets were not smooth, with some ambiguous stripes, which were investigated by using "zigzag triangle" hard mask. A large triangle-mask was employed to investigate smooth facets and the GaN epitaxial behavior. It was found that most of the growth of zincblende GaN was initiated not from A and B-facets but E-facets.

Manuscript submitted August 28, 2013; revised manuscript received October 8, 2013. Published November 13, 2013.

Light-emitting diodes (LEDs) are expected to play an important role in the next-generation light source. Many techniques have been developed for improving internal quantum efficiency and light extraction efficiency of GaN-based LEDs. Patterned sapphire substrate (PSS) is one of these efforts.[1–6]

Two kinds of etching methods have been employed to fabricate PSS: (1) dry etching and (2) wet etching. In wet etching, the sapphire substrate covered with disk-shaped SiO_2 hard mask is usually etched by a mixed solution of hot H_2SO_4 and H_3PO_4. It was found that when the SiO_2 mask still remained on the top c-plane, the PSS structure comprised a hexagonal pyramid covered with six 6B facets $\{13\bar{4}7\}$.[7] It has been found beside normal wurtzite GaN, zincblende GaN has been found on these facets of PSS.[8]

In this study, the exposed facets on PSS structures were investigated by three kinds of SiO_2 hard masks. (1) Rectangle-shaped mask was used to find the smooth facets on PSS structures. (2) Zigzag triangle mask was employed to study the stripes on facets. (3) Triangle mask was used to investigate smooth facets and the zincblende GaN epitaxial behavior.

Experimental

In this study, a 200-nm-thick SiO_2 film served as the wet-etching hard mask and was deposited on the sapphire surface by plasma-enhanced chemical vapor deposition. As shown in Fig. 1 the patterns were in the shape of rectangle (length = 2 μm, width = 0.5 μm) with four orientations (θ = 0°, 15°, 30° and 45°), where θ was the angle between [110] and mask direction. They were denoted as PSS00, PSS15, PSS30 and PSS45, respectively.

Samples were then immersed in a H_3PO_4-based etchant at 270° for 5 and 10 minutes. The surface morphology was analyzed using scanning electron microscope (SEM), and that cross-sectional SEM inspection was achieved after localized etching by focused ion beam (FIB).

Results and Discussion

Sapphire belongs to a rhombohedral crystal system, exhibiting a three-fold rotational symmetry about its c-axis.[9] In the case of three fold symmetry, as illustrated in Fig. 1b, PSS00 (θ = 0°) is equivalent to PSS120 (θ = 120°) and PSS240. Figure 1b also shows that the orientation of PSS60 is the same as that of PSS240, which means PSS60 is equal to PSS00. Therefore, only those angles less than 60° were investigated in this study.

Figures 2a–2d show the SEM images of PSSs after wet etching for 5 minutes. The PSS comprised a 3D structures covered with several facets with a top c-plane. The pattern heights were all about

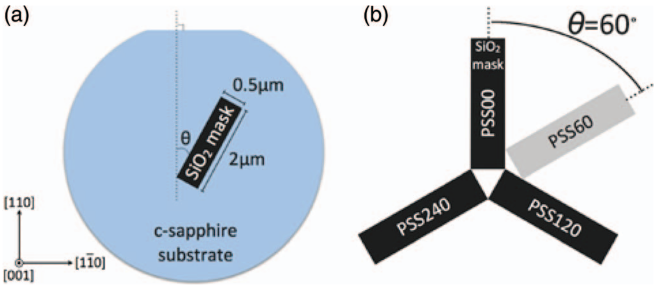

Figure 1. Schematic illustration of (a) rectangle-shaped SiO_2 masks with various orientations and (b) related PSSs.

0.77 μ*m*. The shape of patterns (facets) changed with mask angle. To have more clear view of these facets, samples were etched for 10 minutes as shown in Fig. 2e–2h. The pattern heights were all about 1.69 μ*m*.

The morphologies of these PSSs were schematically illustrated in Fig. 3. They are composed of seven kinds of "facets" in these 3D patterns. They were denoted as A, B, B_1, B_2, D_1, D_2 and E-facet. As illustrated in Fig. 4, there is a mirror plane $(1\bar{2}10)$ on θ = 30°. As a result, the morphologies of PSS45 are the mirror images of PSS15. Therefore, in this study, we only investigate those angles less than 30°.

All A-facets in Fig. 3 were all the same. They have been identified as 6B $\{13\bar{4}7\}$ planes in our previous wet-etched PSS study (Fig. 5), in which disk-shaped SiO_2 mask was used.[7]

Three kinds of B-facets were illustrated in Fig. 3: B, B_1 and B_2. In PSS00, B-facet with triangle shape appeared at left side of the SiO_2 mask. Its surface was smooth. On the other hand, the surfaces of B_1 and B_2-facets were not smooth, with some ambiguous stripes. They were found on PSS15 and PSS30, respectively. Two kinds of D-facets were observed: D_1 and D_2. Stripes were also found on their surfaces. At the same time, E-facets appeared between A and B-facets. Their surfaces were smooth. In other words, A, B and E-facets were smoother than other facets.

To investigate these smooth facets, a large triangle-mask (edge length = 4 μm) was employed to expose these facets. The edges of triangle were parallel to [010], $[\bar{1}\bar{1}0]$ and [100], as shown in Fig. 6. After etching for 15 minutes, three kinds of facets (A, B and E-facet) appeared. The cross-section image (Fig. 6b) shows that the slanted angle between B-facet and bottom c-plane (0001) was 38.9°.

The Miller-Bravais index of B-facet plane was calculated from the intercepts of B-facet plane on the a_1, a_2 and c-axis as illustrated in Fig. 6d.[7] Then, take the reciprocals of these intercepts numbers, and multiplied with sapphire's unit length ($a = 4.759$Å and $c = 12.991$Å).[9] The calculated plane index of B-facet plane was $(10\bar{1}4)$.

[z]E-mail: SermonWu@StanfordAlumni.org

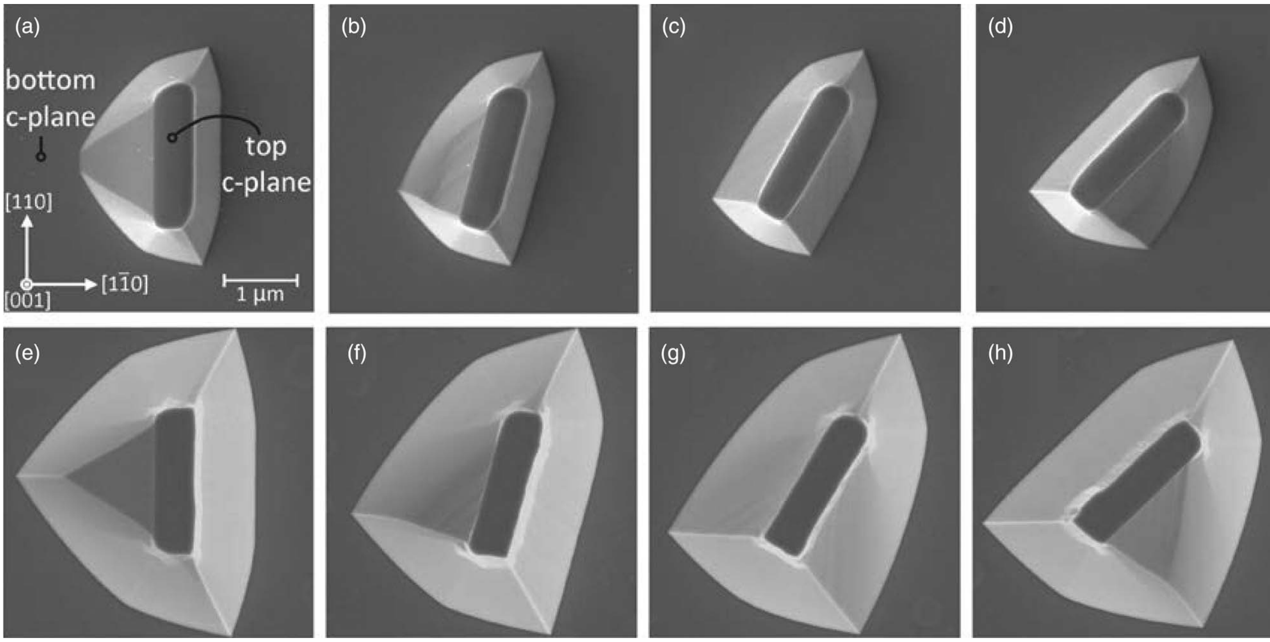

Figure 2. SEM images (SiO_2 masks were removed) of (a) PSS00, (b) PSS15, (c) PSS30 and (d) PSS45 after etching for 5 minutes. (e)-(h) are the related PSSs after etching for 10 minutes.

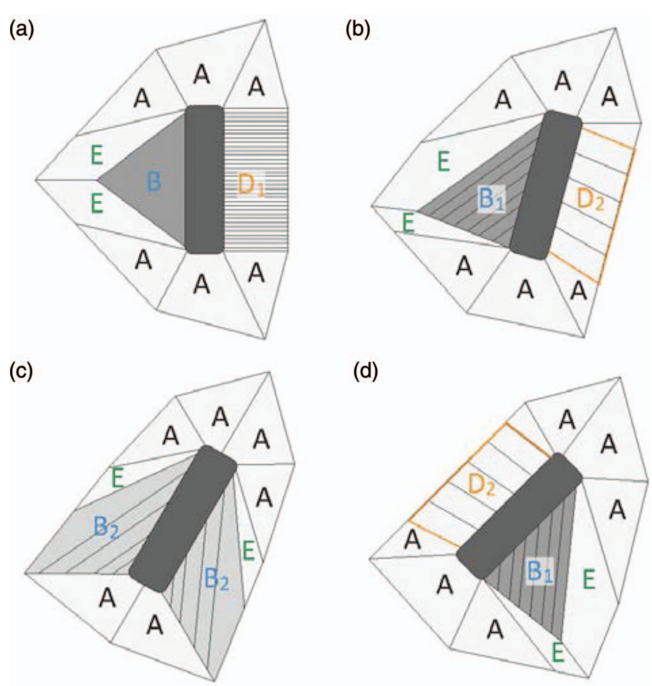

Figure 3. Schematic illustrations of various facets on PSSs: (a) PSS00, (b) PSS15, (c) PSS30 and (d) PSS45.

The B-facet plane index was confirmed by calculating the angle among B-facet and bottom c-plane (0001). The angle, φ, between two crystal planes ($h_1k_1i_1l_1$) and ($h_2k_2i_2l_2$) is given by

$$\varphi = \cos^{-1}\left[\frac{h_1h_2 - (h_1k_2 + h_2k_1)/2 + k_1k_2 + \frac{3a^2}{4c^2}l_1l_2}{\left(h_1^2 - h_1k_1 + k_1^2 + \frac{3a^2}{4c^2}l_1^2\right)^{1/2}\left(h_2^2 - h_2k_2 + k_2^2 + \frac{3a^2}{4c^2}l_2^2\right)^{1/2}}\right]$$

The calculated angle between B-facet plane and bottom c-plane was 38.2°, which was almost the same as the angles observed in Fig. 6b. The Miller-Bravais index of E-facet plane was

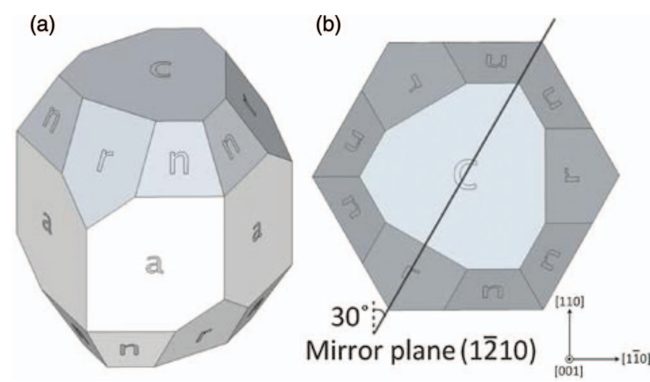

Figure 4. (a) is the crystallographic diagrams of sapphire. (b) is the relative projection of mirror plane $(1\bar{2}10)$ on c-plane (0001).

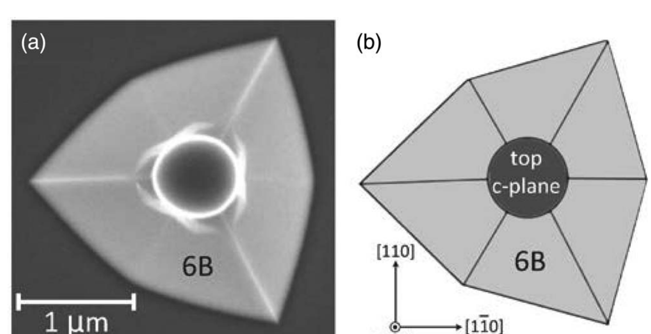

Figure 5. (a) SEM images and (b) schematic illustrations of 6B $\{13\bar{4}7\}$ planes.

hard to be identified due to the small area. However, the intercepts of E-facet plane were estimated. 3D models of related planes ($\{12\bar{3}4\}$, $\{12\bar{3}5\}$, $\{12\bar{3}6\}$, $\{23\bar{5}4\}$ ...) were constructed. After comparing SEM images, their plane indexes might be $\{12\bar{3}5\}$.

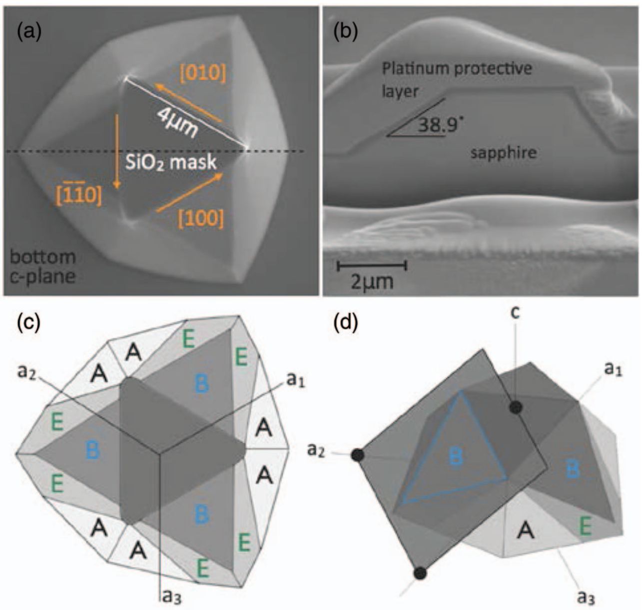

Figure 6. SEM images and schematic illustrations of triangle-PSS after removing of SiO_2. (a) Top-view image. (b) Cross-section image from (a) indicated by dashed line (viewed from 52° to sample normal). (c) Top-view illustration of A, B and E-facets. (d) The intercepts of an "extended" B-facet on a_1, a_2 and c axis.

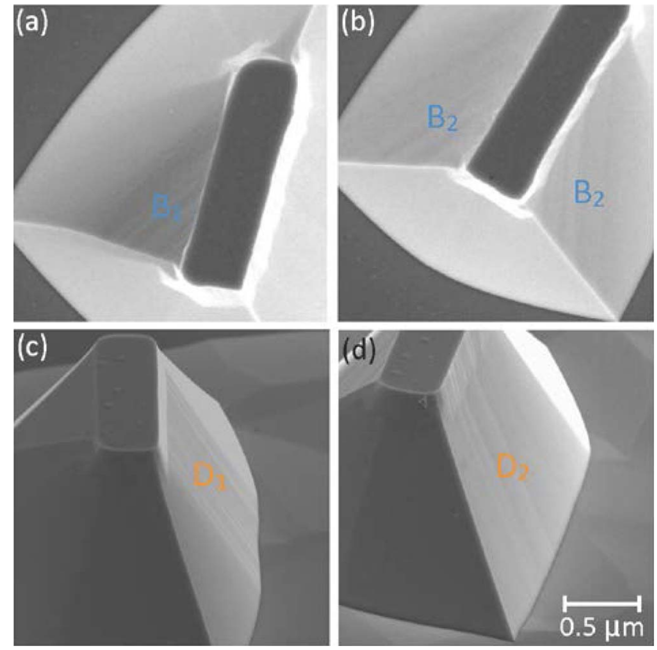

Figure 7. High-magnification SEM images of facets. Top-view images of (a) B_1-facet and (b) B_2-facet. Side-view images of (c) D_1-facet and (d) D_2-facet (viewed from 52° to sample normal).

Fig. 7 was the high magnifications of B_1, B_2, D_1 and D_2-facets. Their zigzag-like surfaces seem to be composed of other facets. In other words, the strips seem to be the border of other facets. To test this model, "zigzag triangle" SiO_2 films were used as wet-etching hard masks, as illustrated in Figs. 8a–8c. The reason why using triangle hard masks is originated from the fact that no strip was found when using triangle mask (Fig. 6). In other words, A, B and E-facets were

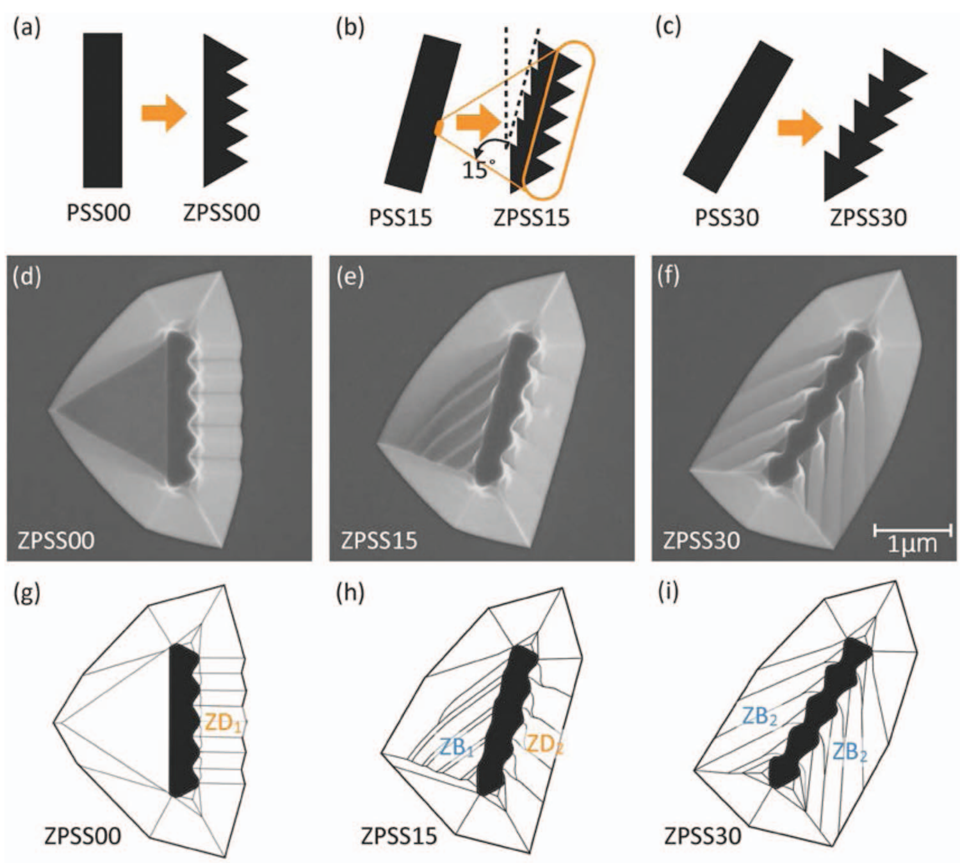

Figure 8. Images and related illustrations of ZPSSs. (a), (b) and (c) are schematic illustrations of masks. (d), (e) and (f) are SEM images of ZPSSs. (g), (h) and (i) are schematic illustrations of ZPSSs.

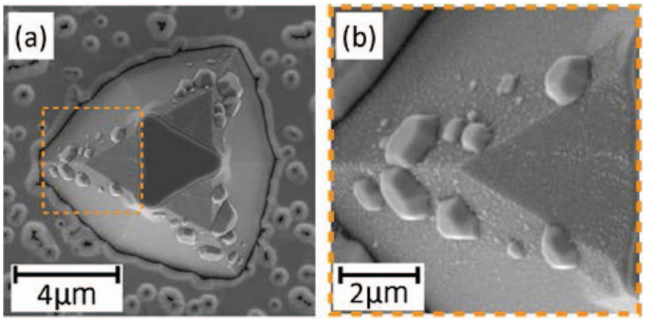

Figure 9. (a) SEM image of GaN grown on triangle-PSS with SiO_2 layer hard mask on top c-plane. (b) The high magnification SEM image from (a) indicated by dashed frame.

smoother than other "facets". B_1, B_2, D_1 and D_2-facets might be composed of A, B and E-facets.

As illustrated in Fig. 6a–6c, these zigzag triangle masks were composed of a stack of five triangles with three different angles to simulate PSS00, PSS15 and PSS30. After etching for 10 minutes, these PSSs were designated as ZPSS00, ZPSS15 and ZPSS30, respectively. The related "facets" were designated as ZB_1, ZB_2, ZD_1 and ZD_2. Their SEM images and schematic illustrations were shown in Figs. 8d–8i. Since the strip orientations on ZB_1, ZB_2, ZD_1 and ZD_2-facets are the same as those on B_1, B_2, D_1 and D_2-facets (Figs. 3 and 7), this model might be true. The ZD_1 and ZD_2-facets might be composed of two different A-facets; ZB_1 might be composed of B and E-facets; ZB_2 might be composed of B, E and A-facets.

To understand the GaN epitaxial behavior on smooth facets (A, B and E-facets), a 700-nm-thick GaN film was grown on the bottom c-plane of large triangle-PSS. Beside bottom c-plane, as shown in Fig. 9, most of the growth of GaN was initiated not from A and B-facets but E-facets. Transmission electron microscopy (TEM) analysis shows these GaN islands are zincblende structures, which are the same as our previous study.[8]

Conclusions

Wet-etched PSS has been used to grow GaN-based LEDs. In wet etching process, several etched facets were exposed on PSS structure. The PSS structure comprised a pyramid covered with several etched facets. In addition to c-plane (0001), zincblende GaN has been found grown on these facets.

In this study, rectangle-shaped SiO_2 hard masks with various orientations were employed to find these facets (A, B, B_1, B_2, D_1, D_2 and E). The surfaces of A, B and E-facets were smooth. Their plane indexes were $\{13\bar{4}7\}$, $\{10\bar{1}4\}$ and $\{12\bar{3}5\}$, respectively. On the other hand, the surfaces of B_1, B_2, D_1 and D_2-facets were not smooth, with some ambiguous stripes, which seem to be the border of A, B and E-facets

Smooth facets (A, B and E) were used to investigate the GaN epitaxial behavior. It was found that most of the growth of zincblende GaN was initiated not from A and B-facets but E-facets.

Acknowledgments

This project was funded by Sino American Silicon Products Incorporation and the National Science Council of the Republic of China under grant No. 101-2221-E-009-052-MY3. Technical support from the National Nano Device Laboratory, Center for Nano Science and Technology, Nano Facility Center and Semiconductor Laser Technology Laboratory of the National Chiao Tung University is also gratefully acknowledged.

References

1. D. S. Wuu, W. K. Wang, W. C. Shih, R. H. Horng, C. E. Lee, W. Y. Lin, and J. S. Fang, *IEEE Photon. Technol. Lett.*, **17**, 288 (2005).
2. Z. H. Feng and K. M. Lau, *IEEE Photon. Technol. Lett.*, **17**, 1812 (2005).
3. Y. J. Lee, T. C. Hsu, H. C. Kuo, S. C. Wang, Y. L. Yang, S. N. Yen, Y. T. Chu, Y. J. Shen, M. H. Hsieh, M. J. Jou, and B. J. Lee, *Mater. Sci. Eng. B*, **122**, 184 (2005).
4. Y. J. Lee, J. M. Hwang, T. C. Hsu, M. H. Hsieh, M. J. Jou, B. J. Lee, T. C. Lu, H. C. Kuo, and S. C. Wang, *IEEE Photon. Technol. Lett.*, **18**, 1152 (2006).
5. K. Tadatomo, H. Okagawa, Y. Ohuchi, T. Tsunekawa, Y. Imada, M. Kato, and T. Taguchi, *J. Jpn. Appl. Phys.*, **40**, L583 (2001).
6. M. Yamada, T. Mitani, Y. Narukawa, S. Shioji, I. Niki, S. Sonobe, K. Deguchi, M. Sano, and T. Mukai, *J. Jpn. Appl. Phys.*, **41**, L1431 (2002).
7. Y. C. Chen, F. C. Hsiao, B. W. Lin, B. M. Wang, Y. S. Wu, and W. C. Hsu, *J. Electrochem. Soc.*, **159**, D362 (2012).
8. J. H. Cheng, Y. S. Wu, W. C. Liao, and B. W. Lin, *Appl. Phys. Lett.*, **96**, 051109 (2010).
9. W. E. Lee and K. P. D. Lagerlof, *J. Electron Microsc. Tech.*, **2**, 247 (1985).